StiFF 2025

Strategic use of stainless steel to improve the performance of steel structures in fire – key findings from the RESIST project

Chunyan Quan, Luke Lapira, Katherine A. Cashell

Research Fellow

University College London (UCL)

26/09/2025

➢ EPSRC funded project – RESIlient buildings using STainless steel (RESIST)

Vision: To bring a step-change in resilience of new and rehabilitated steel buildings by the strategic use of highly ductile elements in key locations

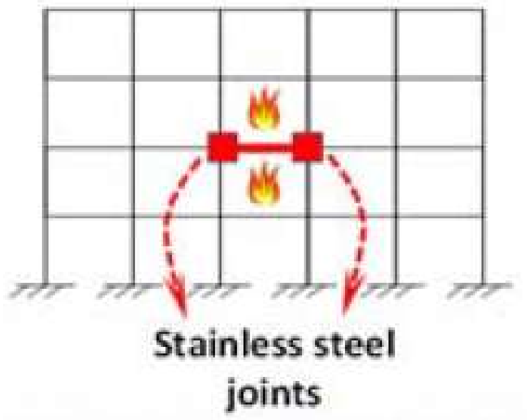

➢ Why stainless steel?

- ✓ Superior corrosion resistance and ductility
- ✓ Enhanced fire resistance

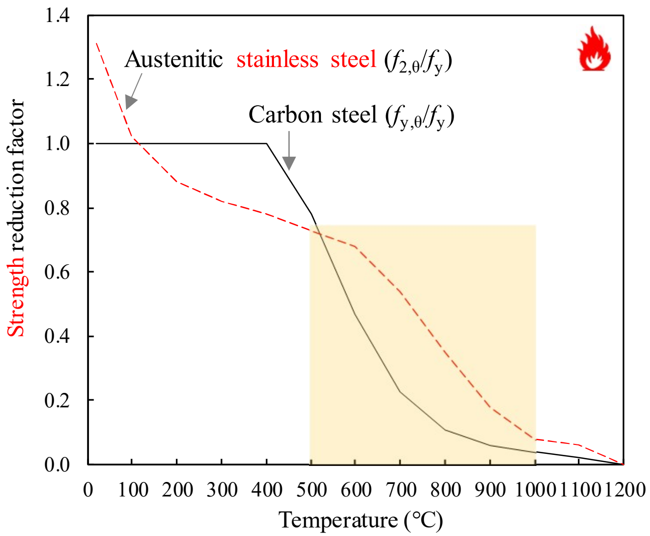

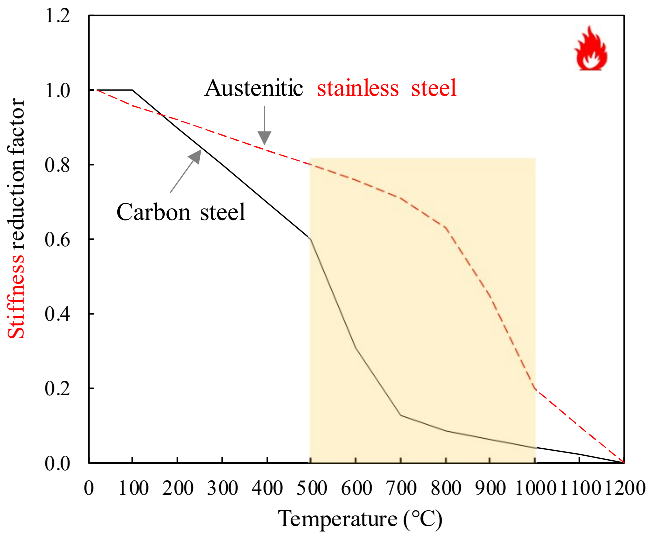

- ➢ **Hybrid**: Replacing carbon steel components in the joint zone with stainless steel.
- ✓ Achieve enhanced performance & optimise cost efficiency

➢ **EPSRC funded project – RESIlient buildings using STainless steel (RESIST)**

IMPERIAL

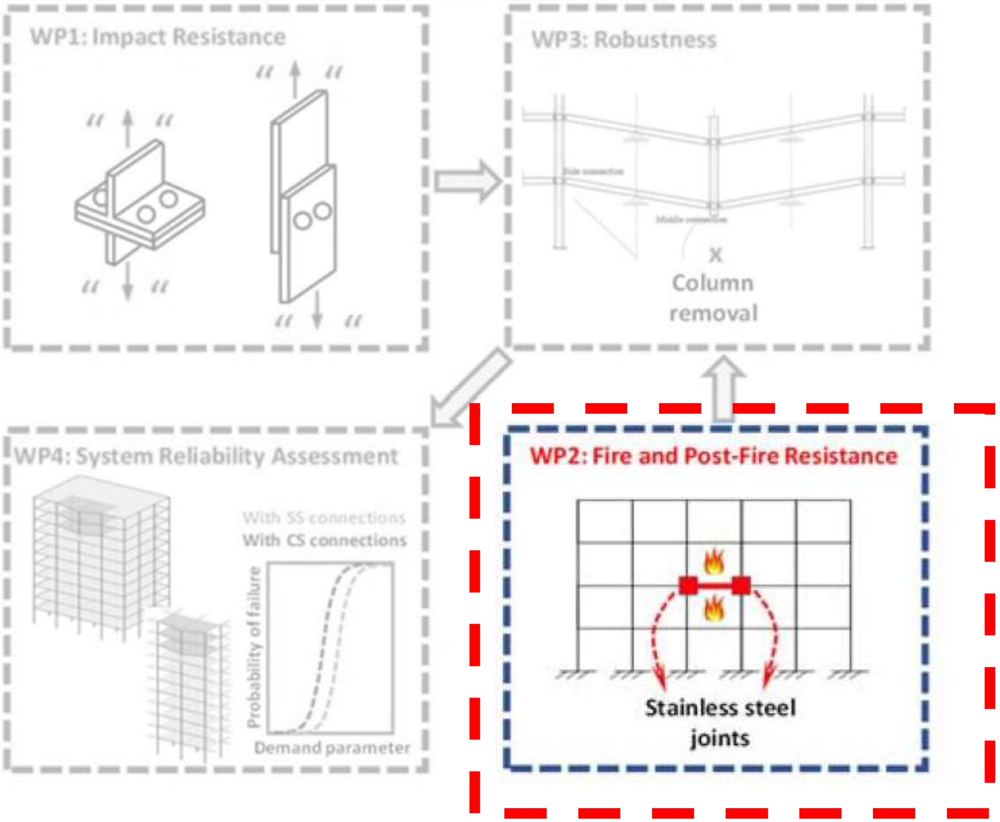

UNIVERSITY OF BIRMINGHAM

University of Southampton

UCL

➢ Research objectives – fire and post-fire

Material properties	Connection behaviour	Design methodologies
Plate	Endplate	Component based method
Bolt	Angle cleat	Advanced models for T-Stubs

Material properties

➢ Post-fire material tests on stainless steel H500 (nickel-free) plates

- **46 coupon specimens heated in furnace.**
  - Heated at a rate of **10 °C/min**.
  - Exposed to the target temperature for **20 minutes**.
- **Two cooling techniques**
  - Cool in **water** (CIW) in a metal bucket.
  - Cool in **air** on top of a brick.

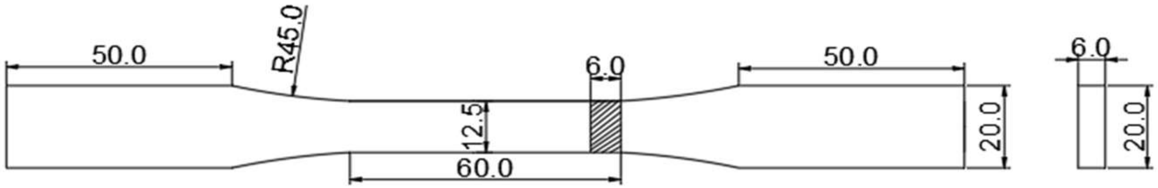

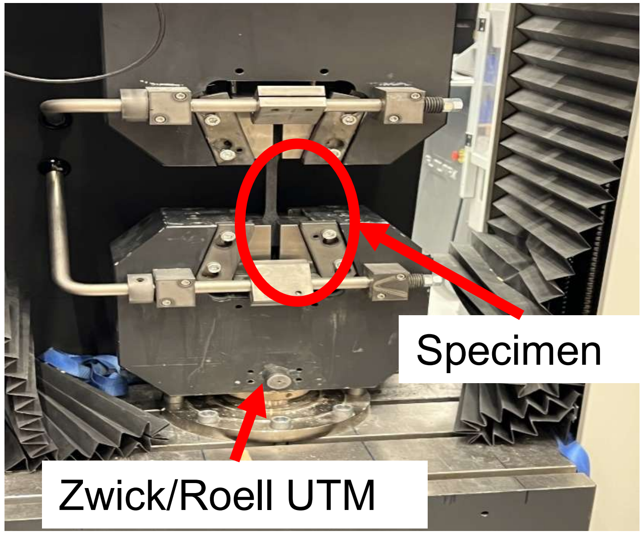

Test setup

MATERIAL PROPERTIES

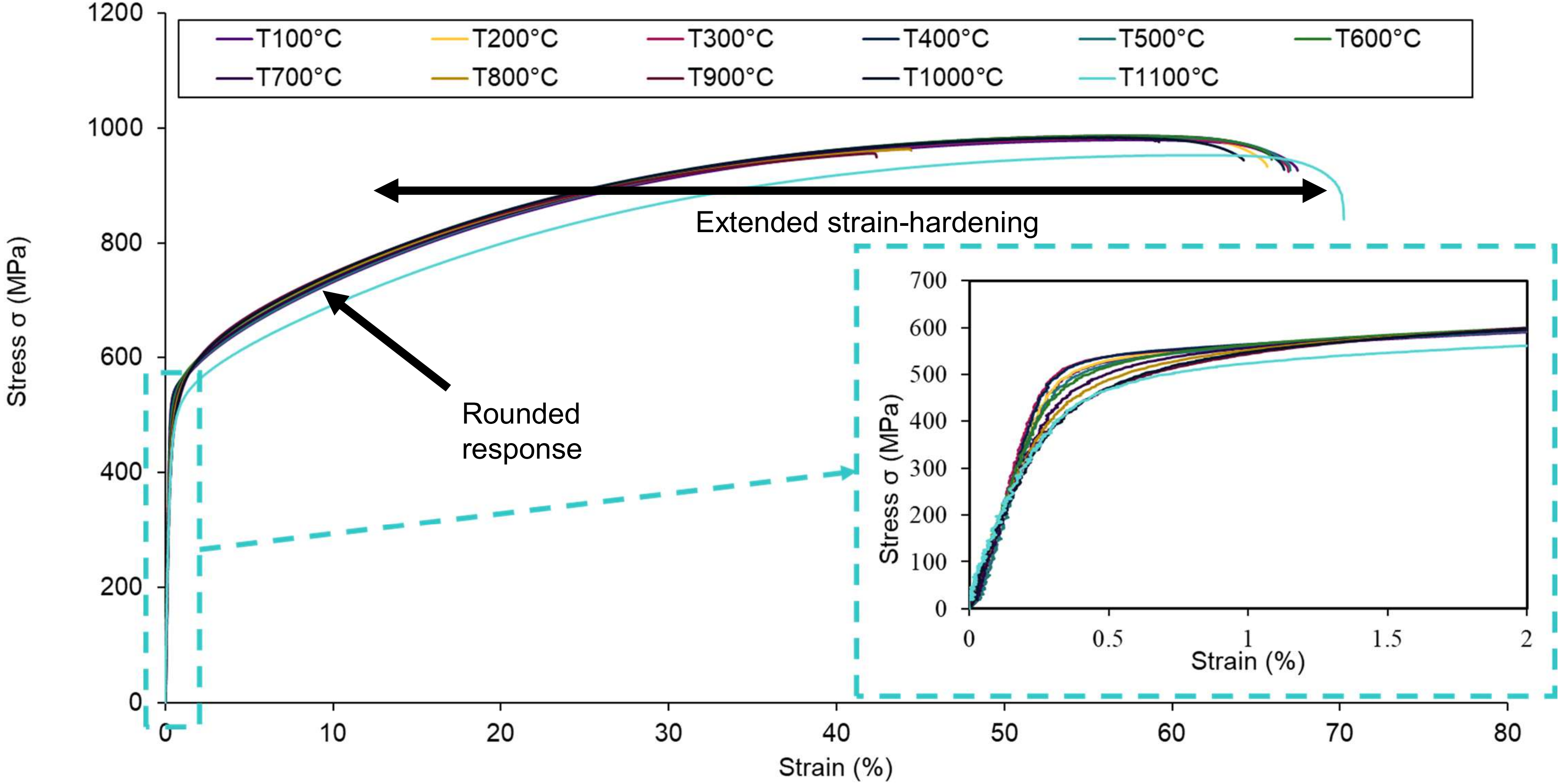

Post-fire stress-strain curve cooled in water (CIW)

➢ **Post-fire mechanical properties**

Mechanical properties

Temperature θ (°C)	E_θ (MPa)	$f_{0.2p,\theta}$ (MPa)	$f_{1.0p,\theta}$ (MPa)	$f_{1.5p,\theta}$ (MPa)	$f_{2p,\theta}$ (MPa)	$f_{u,\theta}$ (MPa)	$\varepsilon_{u,\theta}$ (%)	$\varepsilon_{f,\theta}$ (%)
20	194764	525	570.3	585.6	600	979.1	57.2	65.1
100	203239	524.1	568.4	584.5	598.6	979.2	57.4	67.5
200	199021	524.8	572.5	588.5	603.3	986.4	57.4	65.7
300	198709	534.4	573.2	586.6	600.5	982.1	56.6	66.9
400	196403	539.6	574.3	591	604	986.6	57.6	66.7
500	177337	521.2	572.8	588.2	601.6	984.4	57.6	67
600	176701	517.6	578.6	594.8	608.3	986.2	56.7	65.9
700	157387	503.7	574.5	591	605.6	983.6	55.9	59.2
800	160330	492.2	573.6	593.5	610	963.1	44.2	44.5
900	151860	475.7	567.5	595.5	613.8	955.8	42.1	42.4
1000	148272	482.1	573.3	594.6	610.2	983.3	56.1	64.3
1100	135433	475.6	541.4	559.9	572.6	952.7	61.2	70.2

Stiffness regained

Stiffness loss

➢ Failure modes

Ductile failure with necking

T = [20 – 600 °C],

T = [1000-1100 °C]

Necking

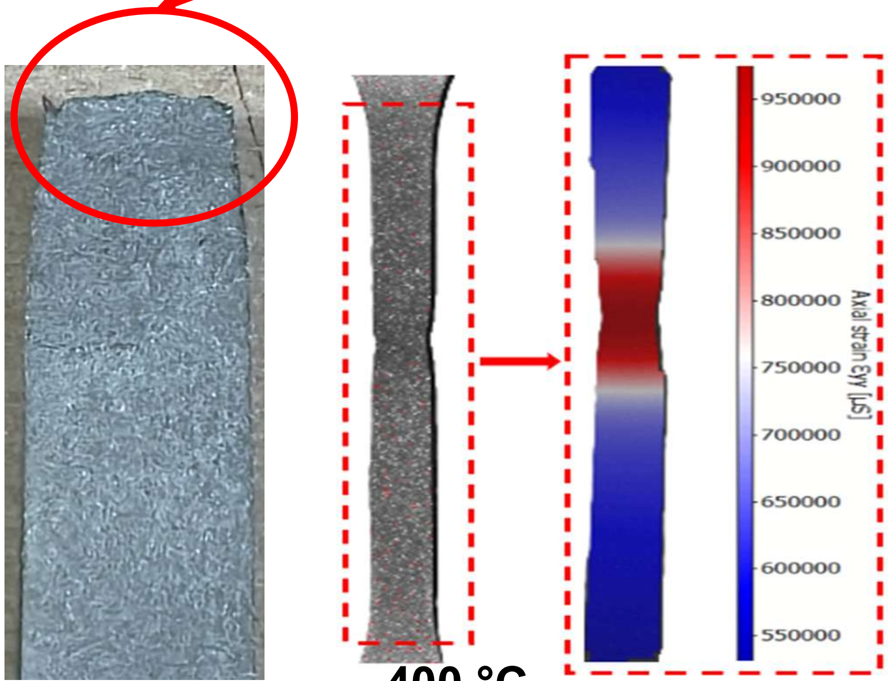

400 °C

Sudden brittle failure

T = [700 – 900 °C]

No signs of necking

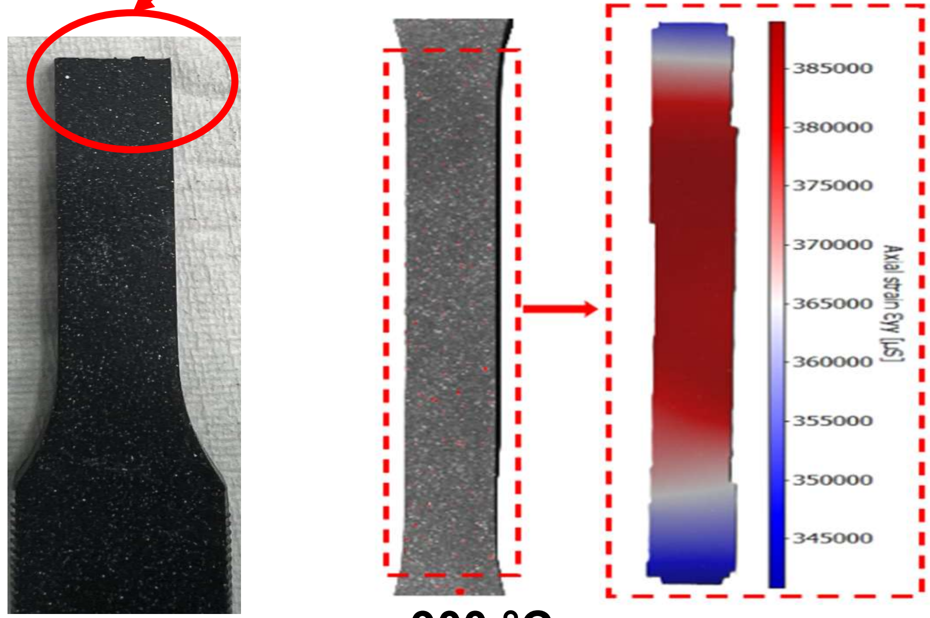

900 °C

➢ Microstructural tests

- **XRD** (X-ray diffraction)

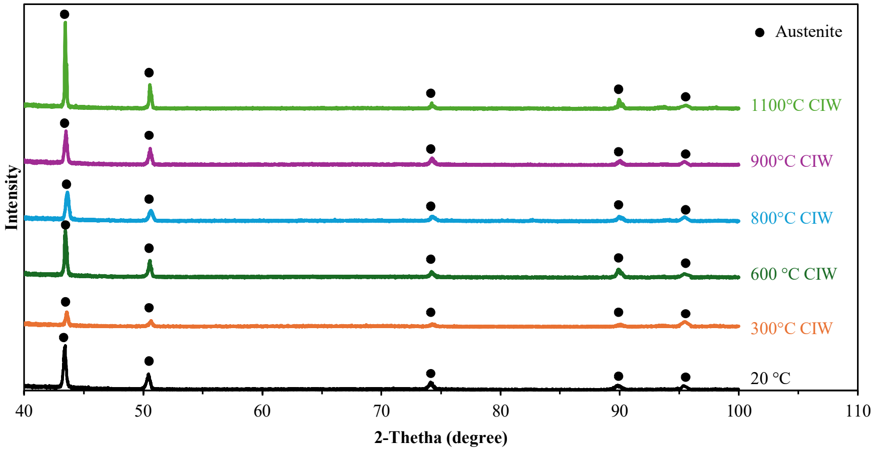

➢ **No notable difference between ductile and brittle specimens**

- **EBSD** (electron backscatter diffraction)

Small grain sizes

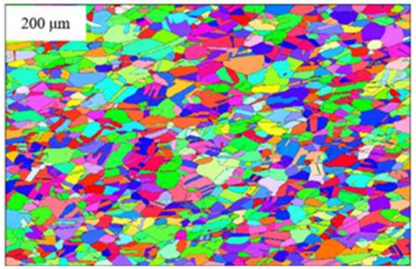

(a) 20 °C

Slight increase in grain sizes

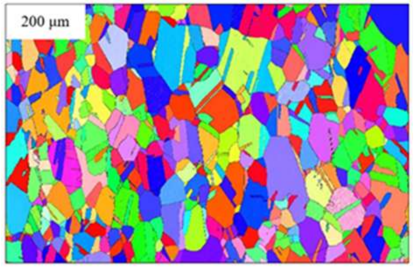

(b) 600 °C

Larger grain sizes

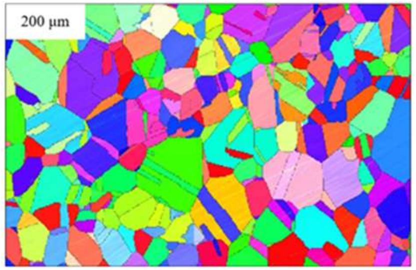

(c) 1100°C

- **EDX** (energy dispersive x-ray)

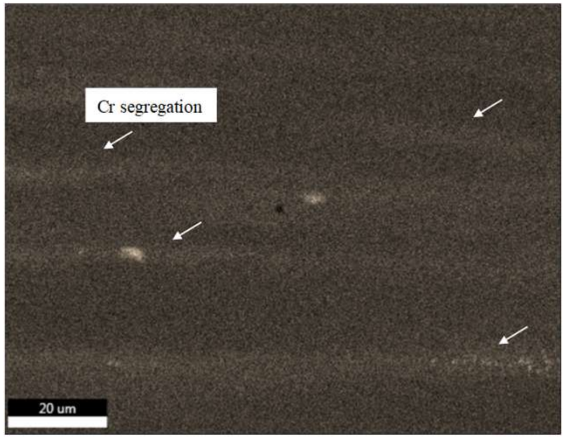

(a) Chromium EDX maps

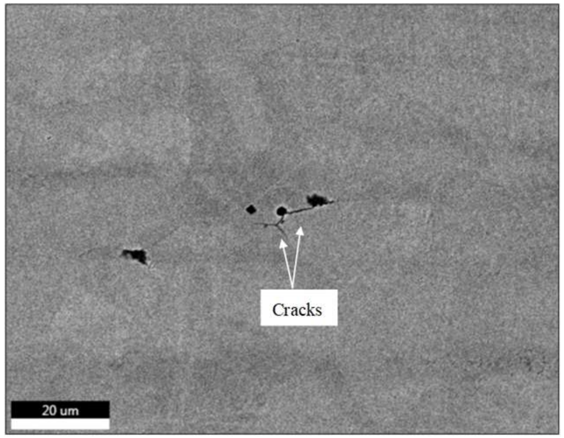

(b) SEM (scanning electron microscopy)

➢ Fracture of stainless steel plates and bolts

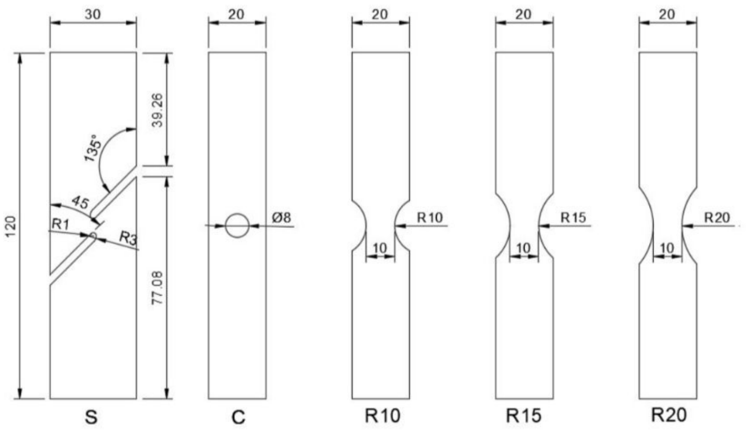

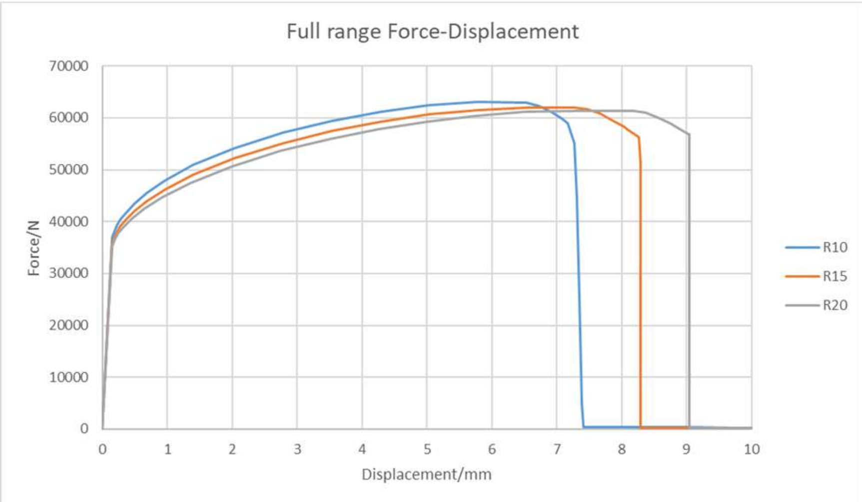

Centre Coupon (from M16 bolt)

Edge Coupon (from M16 bolt)

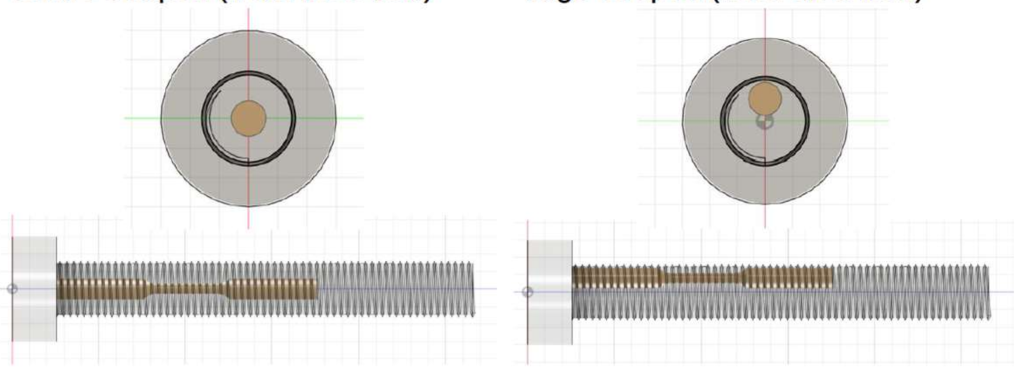

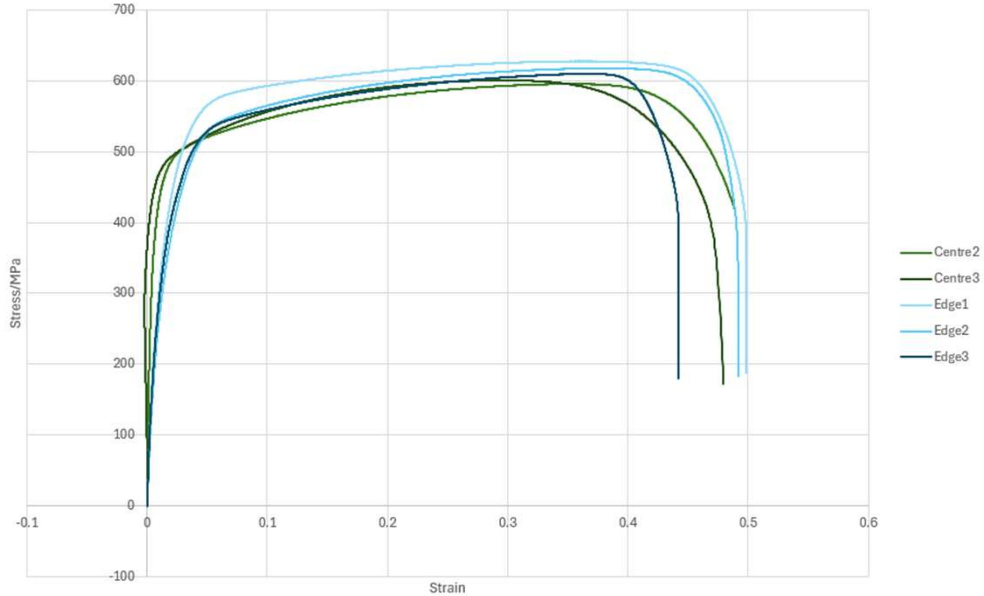

Connection behaviour

➢ FE modelling in ABAQUS

- C3D8R Brick Elements

- EC3 Material models
- Four-stage model
  - Carbon steel
- Two-sage Ramberg-Osgood model
  - Stainless steel plates
  - High-strength steel plates
  - Bolts

- Three static load steps:
  - Bolt preload
  - Uniform heating
  - Displacement controlled loading

Four-stage model

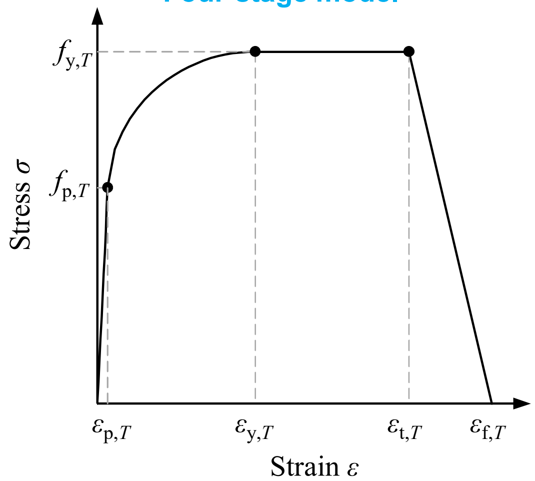

Two-stage Ramberg-Osgood model

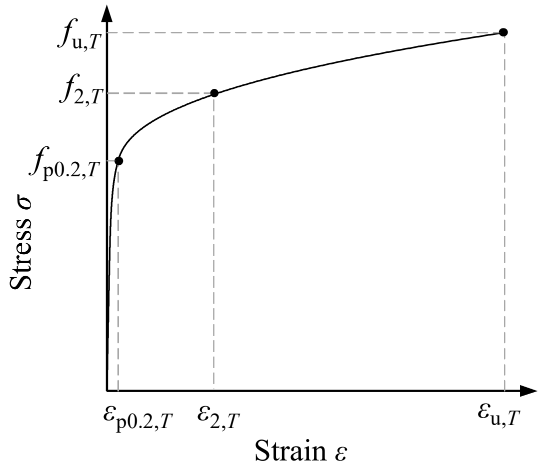

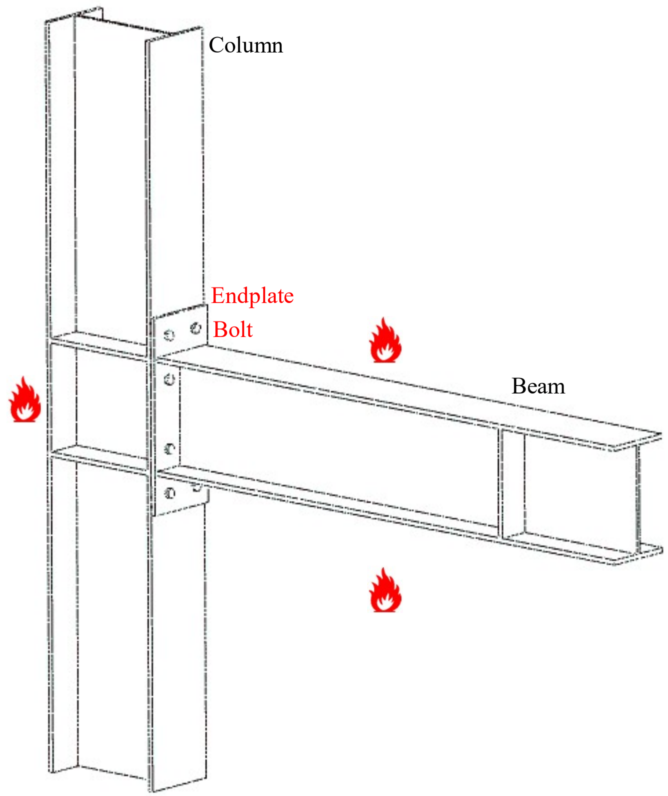

➢ FE modelling in ABAQUS

- **Mechanical strain attains fracture strain**
  - Plates: at any point
  - Bolts: average strain

- **First occurring failure among:**
  (i) plate failure $M_{u,plate}$
  (ii) bolt failure $M_{u,bolt}$
  (iii) peak point in M-θ curve $M_{u,max}$

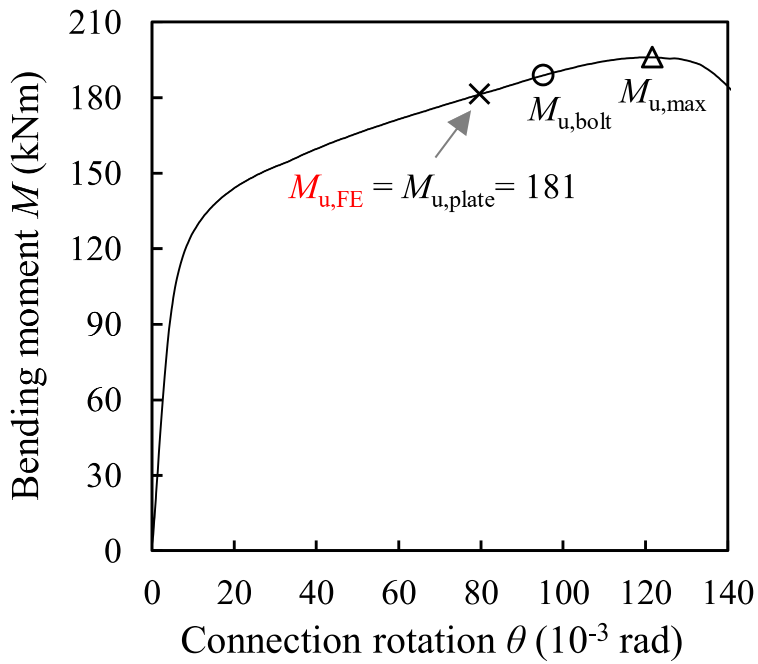

➢ Validation study (endplate)

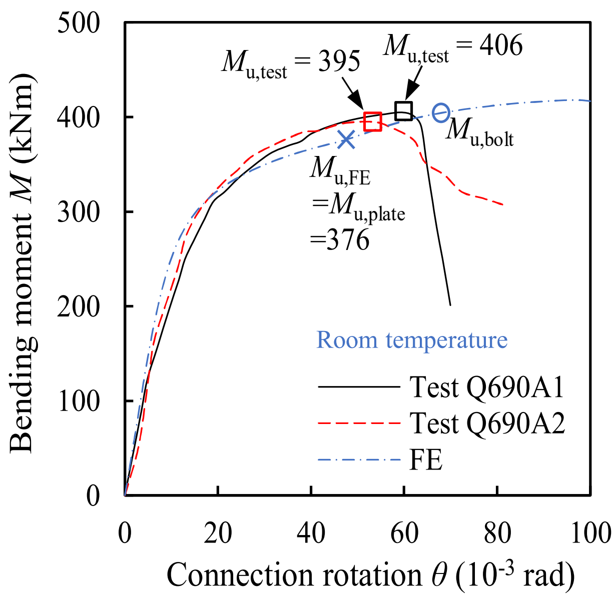

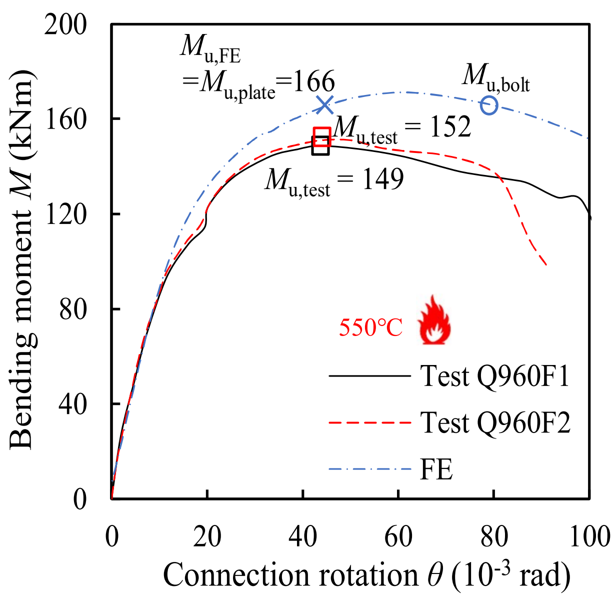

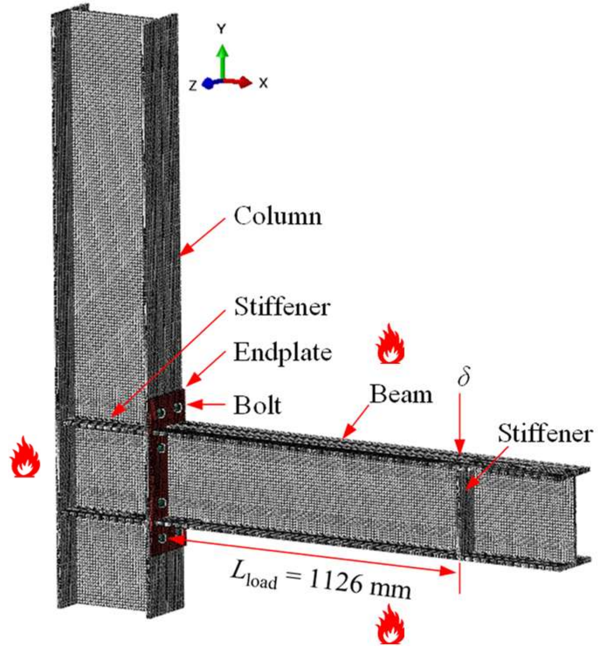

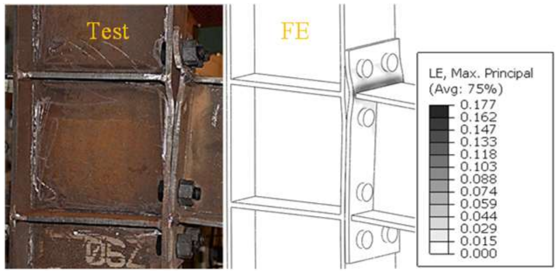

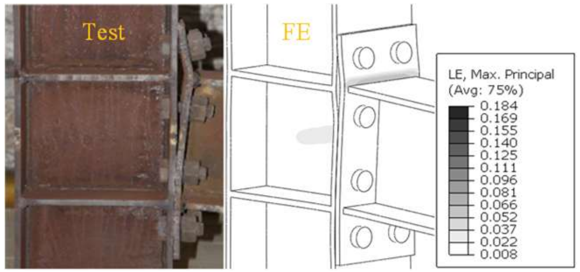

- **High-strength steel endplate connections at 20℃ and 550℃:** Qiang, Wu, Jiang, Luo & Bijlaard 2018, Int. J. Steel Struct. 18: 1350–1362

➢ Validation study (angle cleat)

Top and bottom angle cleats

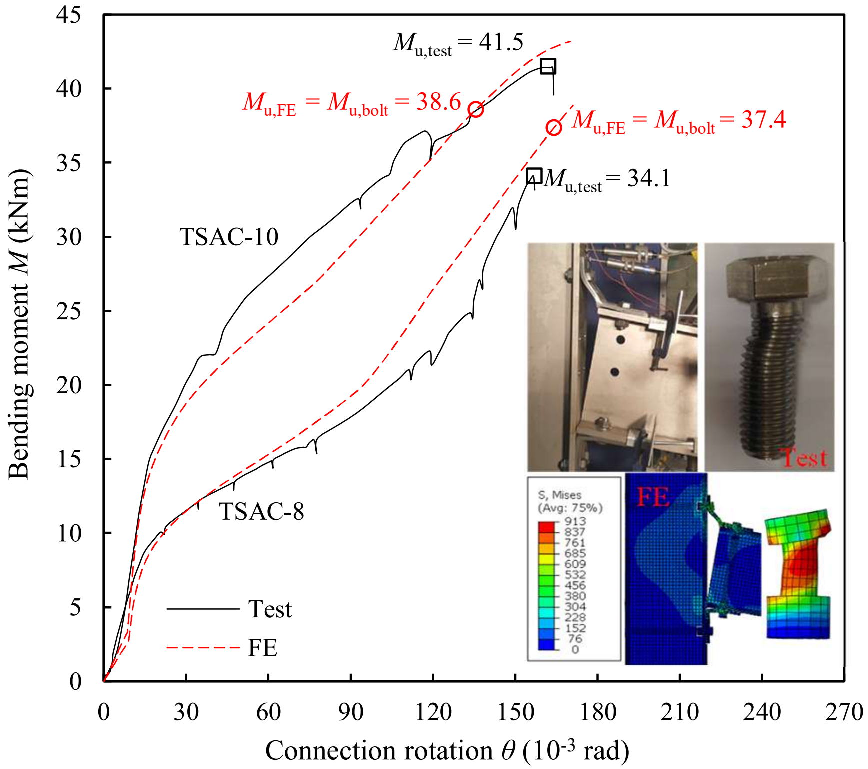

Top and bottom with double web angle cleats

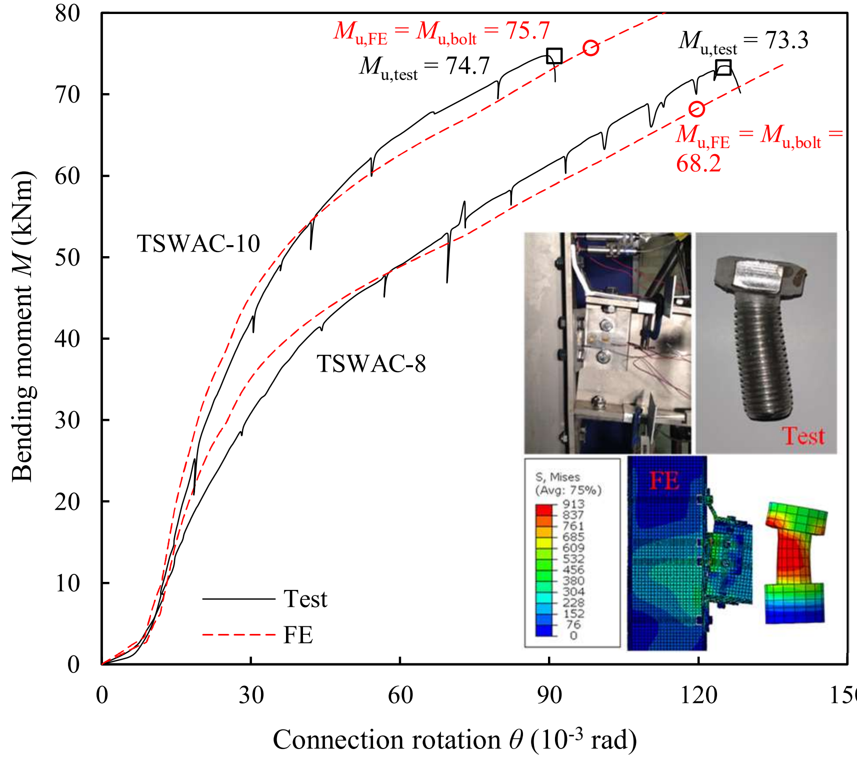

- **Stainless steel angle cleat connections at room temperature:** Elflah, Theofanous, Dirar & Yuan 2019, J. Constr. Steel Res. 152: 183–193

Parametric study (endplate)

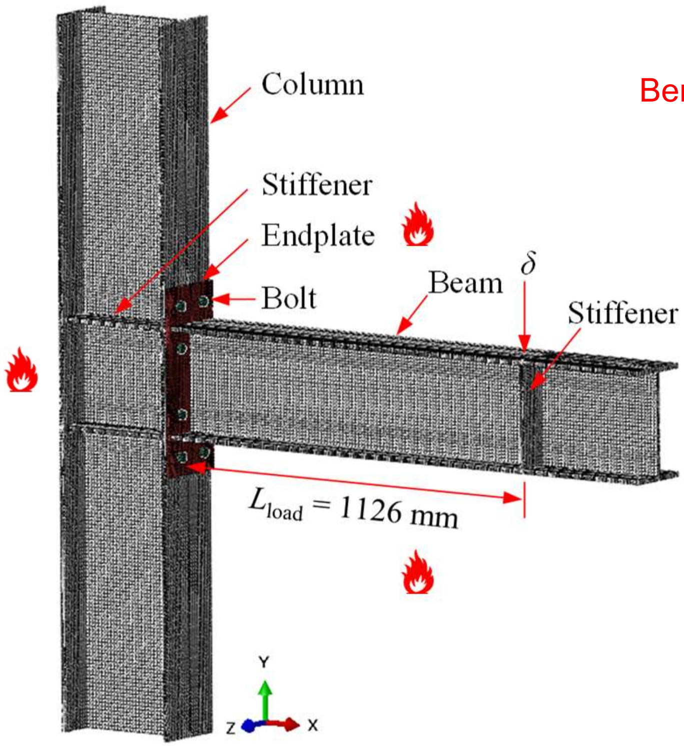

- **56 cases**

	No.	Endplate material	Endplate thickness (mm)	Bolt material	Bolt size	Temperature (℃)
Benchmark	1	S355	12	G8.8	M20	20, 300, 500, 700
	2	S690	12	G8.8	M20	
	3	A1.4420	12	G8.8	M20	
	4	D1.4410	12	G8.8	M20	
	5	F1.4509	12	G8.8	M20	
	6	S355	12	G10.9	M20	
	7	S355	12	A4-70	M20	
	8	A1.4420	12	A4-70	M20	
	9	D1.4410	12	A4-70	M20	
	10	F1.4509	12	A4-70	M20	
	11	S355	10	G8.8	M20	
	12	S355	15	G8.8	M20	
	13	S355	12	G8.8	M16	
	14	S355	12	G8.8	M24	

➢ Parametric study (endplate)

Bolts: G8.8 and stainless steel A4-70

Endplates: S355, austenitic A1.4420, duplex D1.4410 and ferritic F1.4509 stainless steel

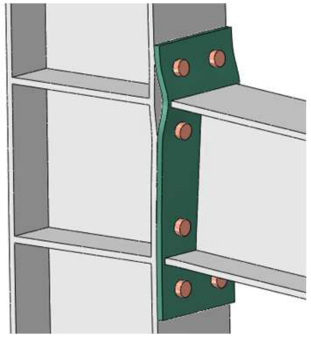

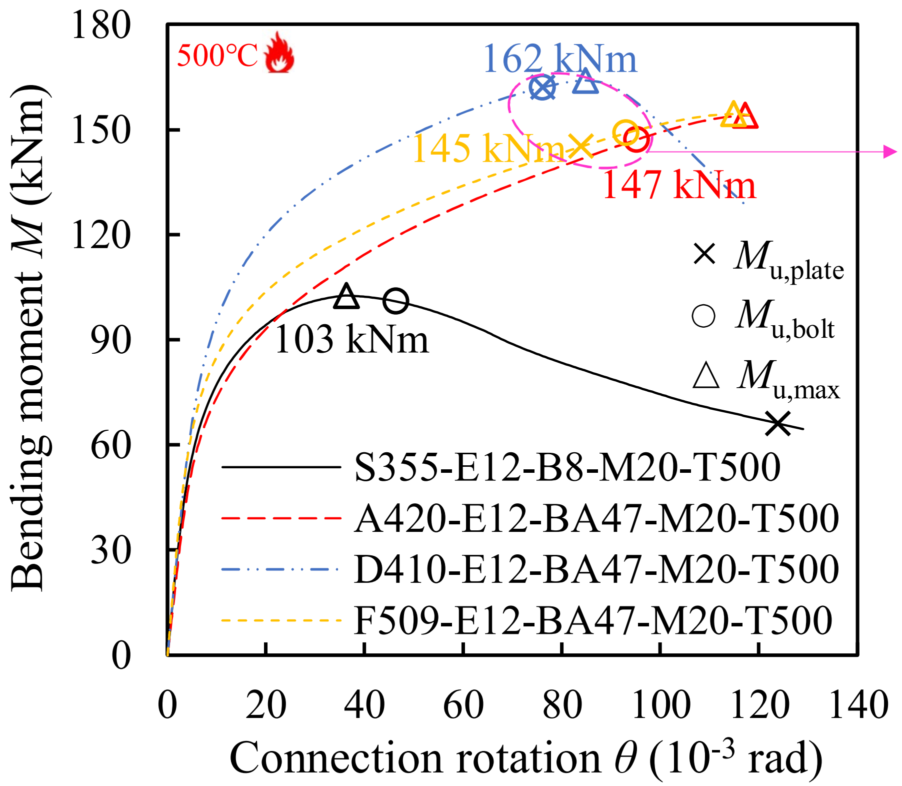

Hybrid connections: **significantly improved ultimate resistances and rotation capacities,** highlighting the advantages of hybrid connections for fire-resistant design.

➢ Parametric study (endplate)

Endplates: S355, S690, austenitic A1.4420, duplex D1.4410 and ferritic F1.4509 stainless steel

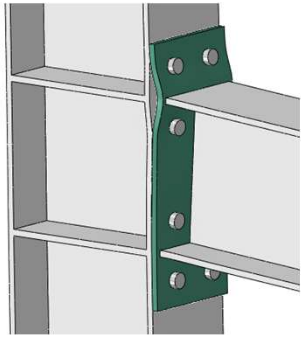

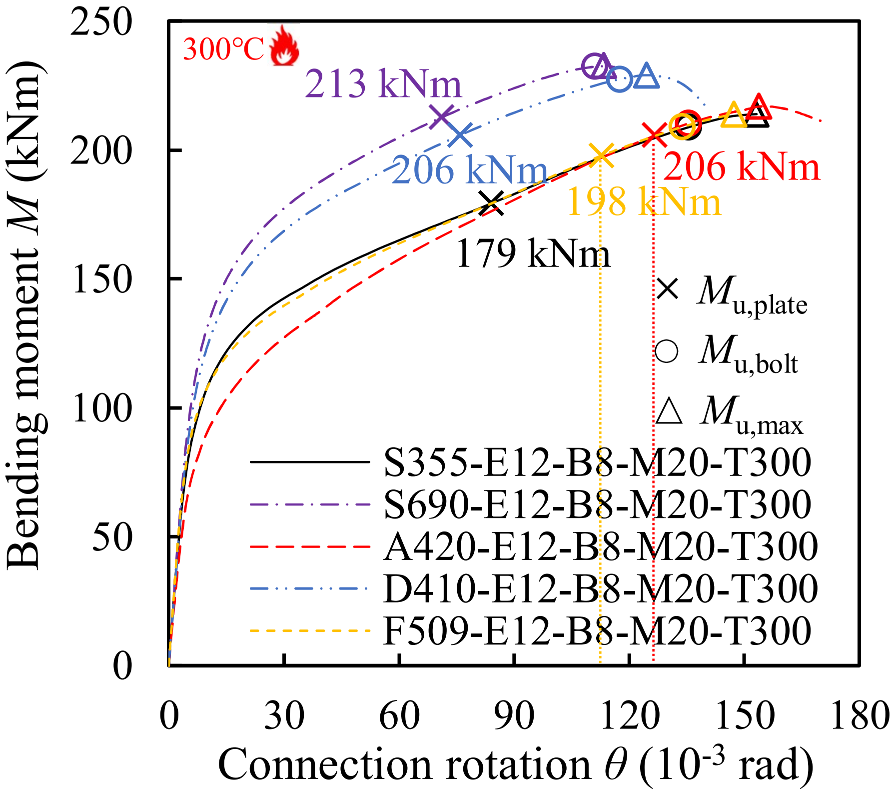

- Hybrid connections: **improved ultimate resistance**, owing to higher material strength.
- A1.4420 and F1.4509: **improving rotation capacity**, owing to greater material ductility.

➢ Parametric study (endplate)

Bolts: G8.8, G10.9 and stainless steel A4-70

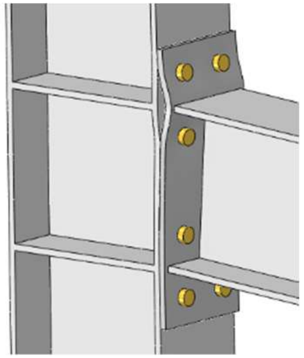

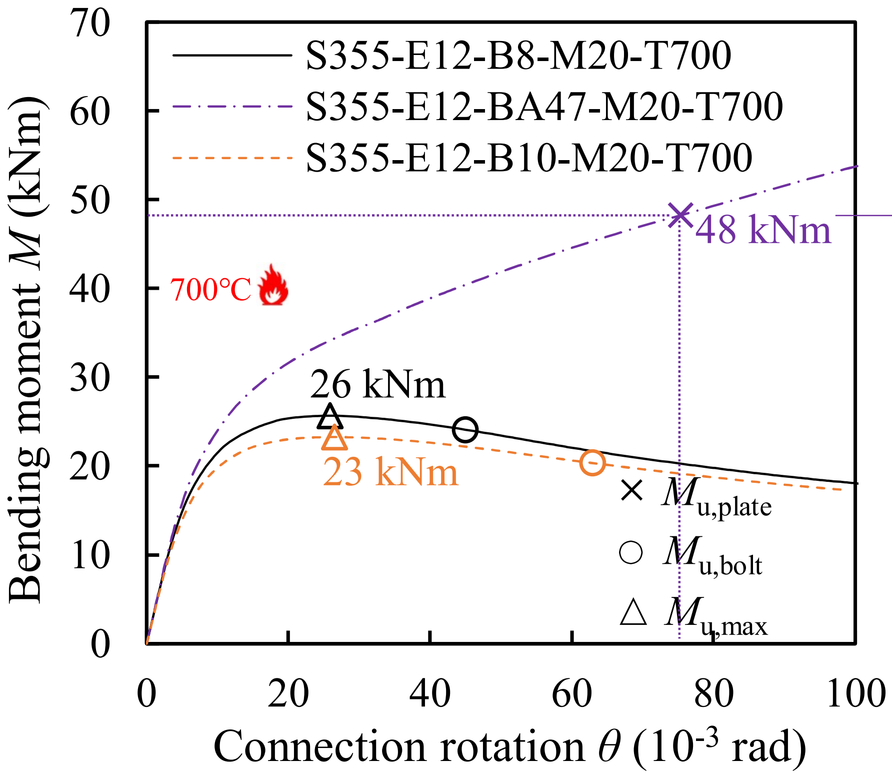

Hybrid connection: **greater ultimate resistance and rotation capacity**, owing to superior strength and ductility.

Parametric study (angle cleat)

- Top and bottom angle cleats (TB)
- Top and bottom with double web angle cleats (TBW)

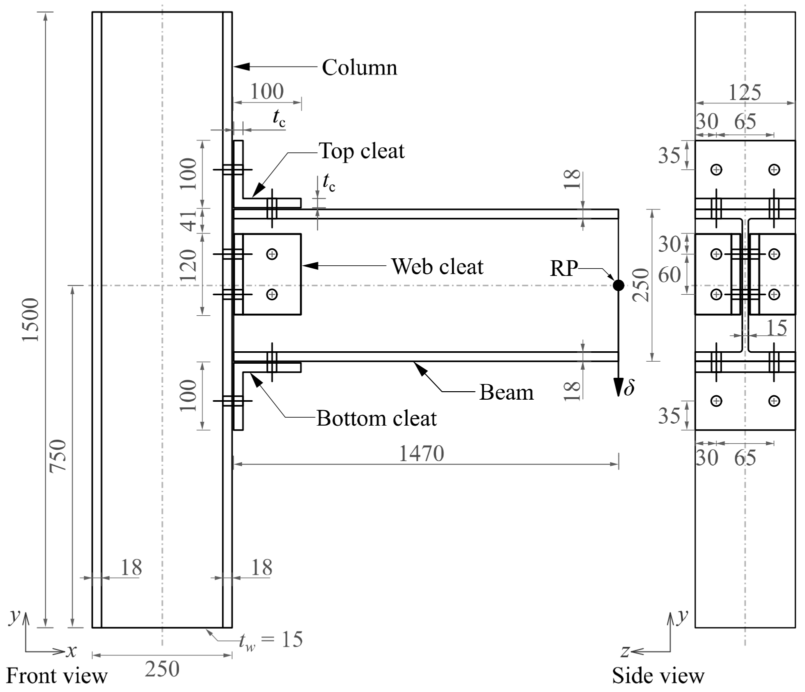

104 cases in total

Parameter		Variables	Benchmark (B)
(i)	Cleat material	S355, S690, H500, D1.4410, F1.4509	S355
(ii)	Bolt material	G8.8, A4-70	G8.8
(iii)	TB Cleat thickness (mm)	10, 12, 15	12
	TBW Cleat thickness (mm)	6, 8, 10	8
(iv)	Bolt size	M12, M16, M20	M16
(v)	Temperature (°C)	20, 300, 500, 700	(all)

➢ Parametric study (angle cleat) – Benchmark case

Room temperature, angle cleat critical

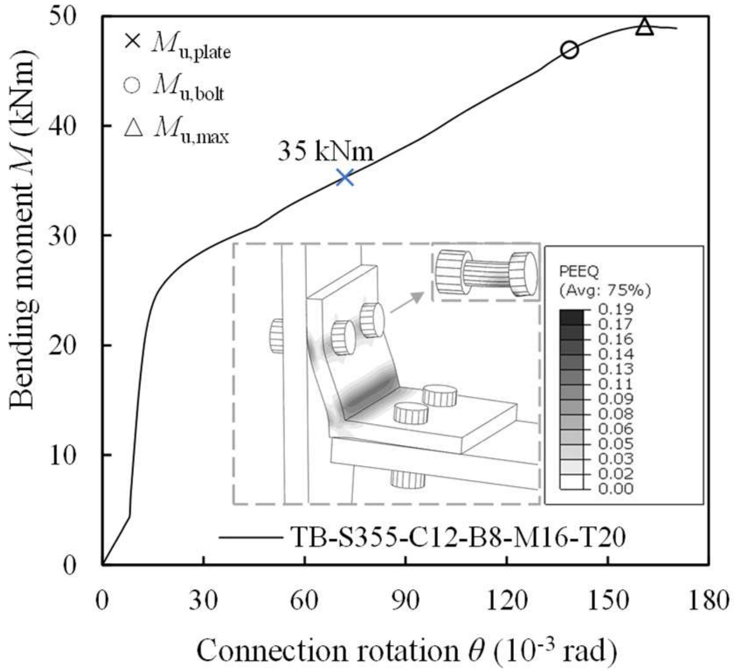

500℃, bolt critical

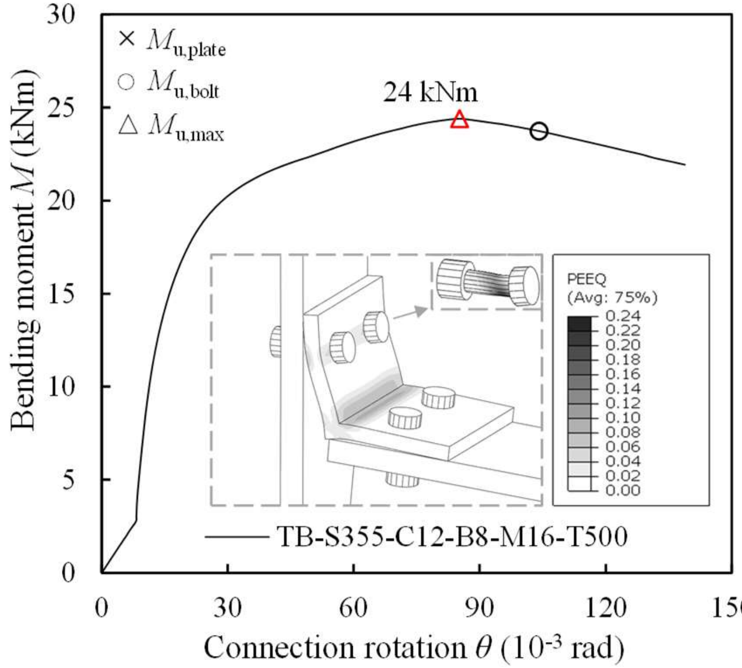

➢ Parametric study (angle cleat)

Bolt material grades
G8.8, stainless steel A4-70

Angle cleat material grades
S355, austenitic H500, duplex D1.4410
ferritic F1.4509

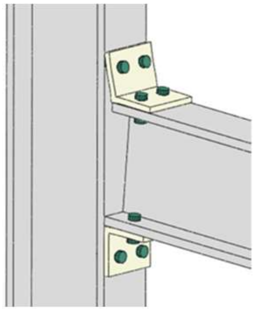

- **Stainless steel bolts:**
  - Improve ultimate resistance
- **Stainless steel angle cleats and bolts:**
  - Significantly improve ultimate resistance
  - May increase rotation capacity

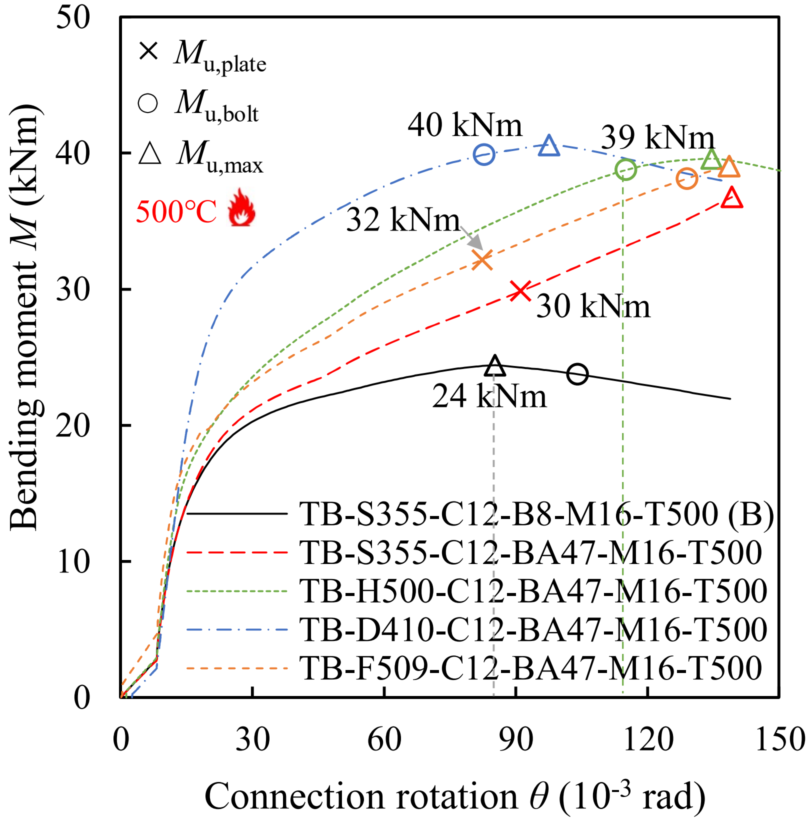

➢ Parametric study (angle cleat)

- **Hybrid connections** improve ultimate strengths **on average:**

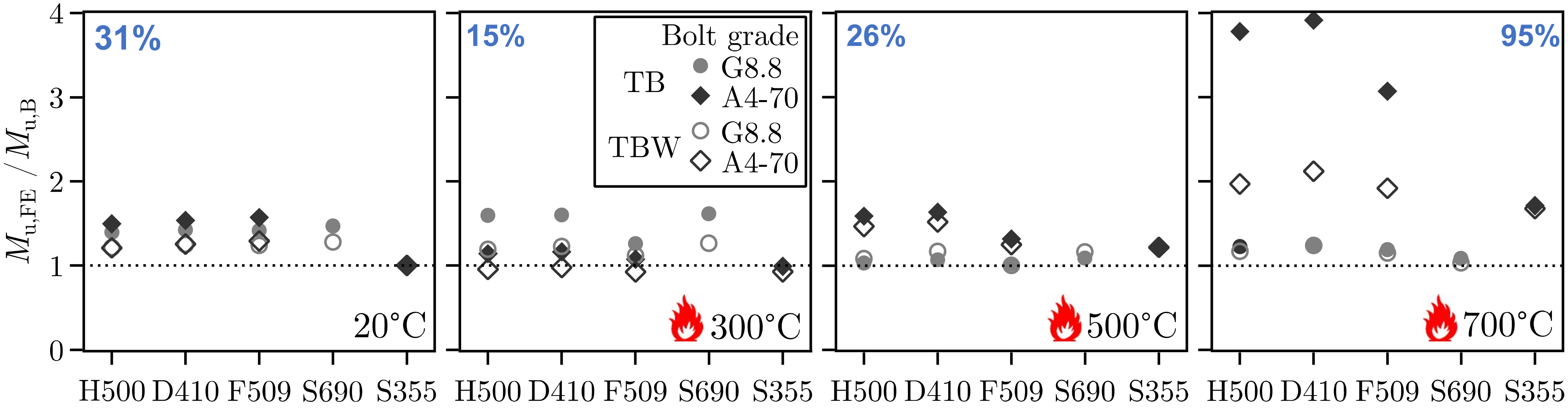

Design methodologies

➢ Endplate connections

EN 1993-1-8:2024 provides component-based method (CBM): connection → springs → individual components.

Tension zone

Shear zone

Compression zone

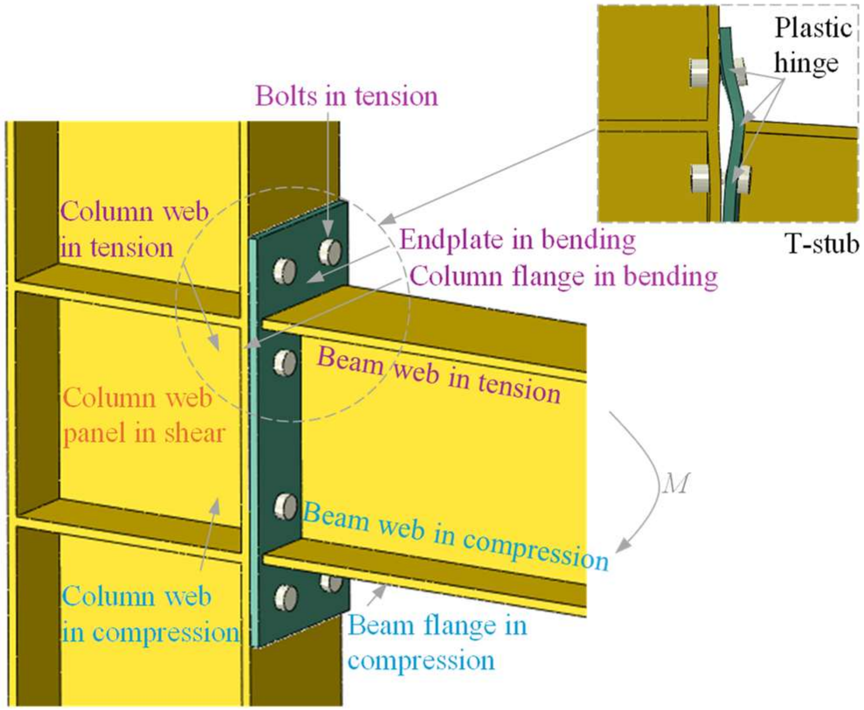

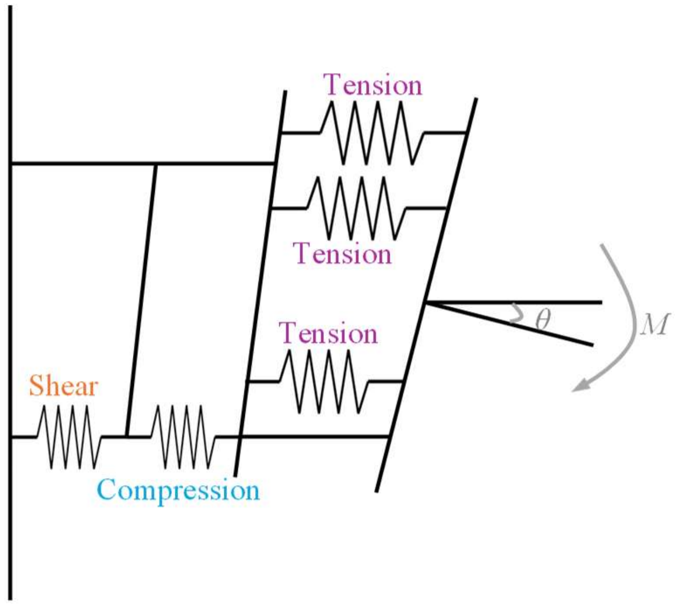

Endplate connections

- **Component-based method**

✓ Room temperature design

? Extended to elevated temperature design

✓ Initial stiffness K_{ini}, calculated using E_T

$$K_{ini} = \frac{z_{eq}^2}{\frac{1}{k_{eq}} + \frac{1}{k_c} + \frac{1}{k_v}}$$

z_{eq} → equivalent lever arm; k_{eq} → all bolt rows; k_c → compression zone; k_v → shear zone

✓ Plastic resistance M_y, calculated using $f_{2,T}$

$$M_y = \sum_i F_i h_i$$

F_i → tension resistance of the bolt row; h_i → distance of the bolt-row from the compression centre

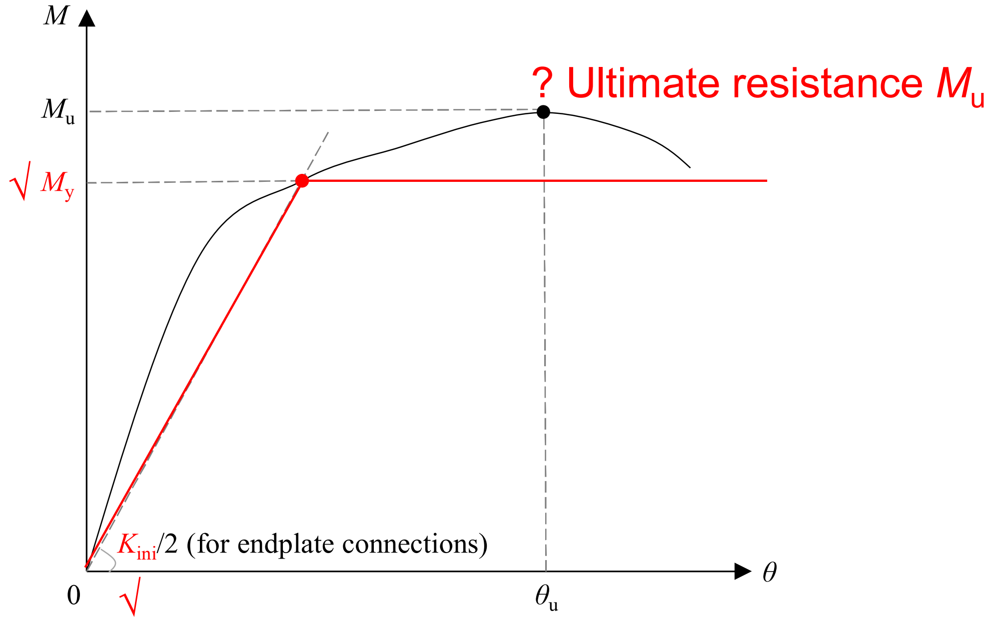

Endplate connections

✓ Ultimate resistance M_u

shape parameter, negligible influence and taken as 0 for endplate connections (Yee & Melchers, 1986)

$$M = M_y \left\{ 1 - \exp\left[\frac{-(K_{ini} - K_p + c\theta)\theta}{M_y} \right] \right\} + K_p\theta$$

(Yee & Melchers, 1986)

Proposal: $$M = M_y \left\{ 1 - \exp\left[\frac{-0.98 K_{ini}\theta}{M_y} \right] \right\} + 0.02 K_{ini}\theta$$

0.02 of K_{ini}, reasonable fit to steel connection data (Jing 2004)

✓ Rotation limit θ_u

elevated temperature effect — material grade effect

$$\theta_u = 0.05\ \text{rad} \times \varepsilon_{u,T} / \varepsilon_{u,basic} = 0.05\ \text{rad} \times k_{\varepsilon u,T}\, \varepsilon_u / \varepsilon_{u,basic}$$

$\varepsilon_{u,T}$: elevated temperature ultimate strain of the critical element

$\varepsilon_{u,basic}$: room temperature ultimate strain of the basic material grade for the same element (G8.8 for bolts and S355 for plates)

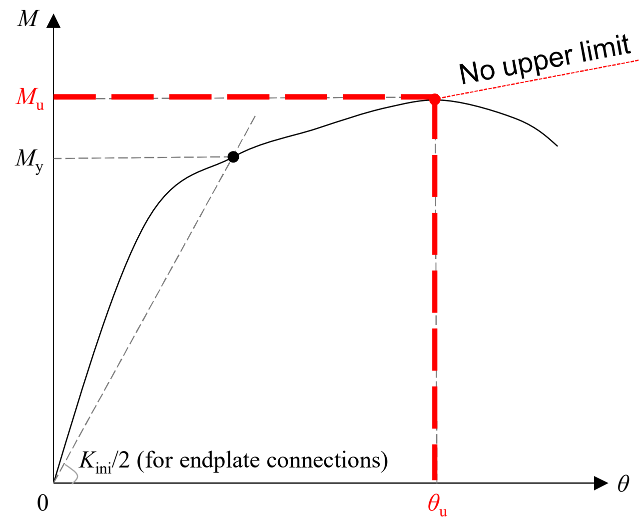

➢ Endplate connections

✓ Application

- **Summary of parametric studies (56 cases in total)**

	$K_{ini,pre}/K_{ini,FE}$	$M_{y,pre}/M_{y,FE}$	$M_{u,pre}/M_{u,FE}$
Mean	0.84	0.93	0.77
CoV	0.064	0.090	0.074
Max	0.96	1.09	0.88
Min	0.70	0.76	0.60

✓ $M_{y,pre}$ are accurate and safe.

✓ $K_{ini,pre}$ and $M_{u,pre}$ are slightly conservative.

✓ The conservatism in $M_{u,pre}$ is partly due to the conservatism in the predicted $K_{ini,pre}$ and $M_{y,pre}$.

✓ $\theta_{u,pre}$ accounts for the reduction in rotation at elevated temperatures.

➢ Angle cleat connections

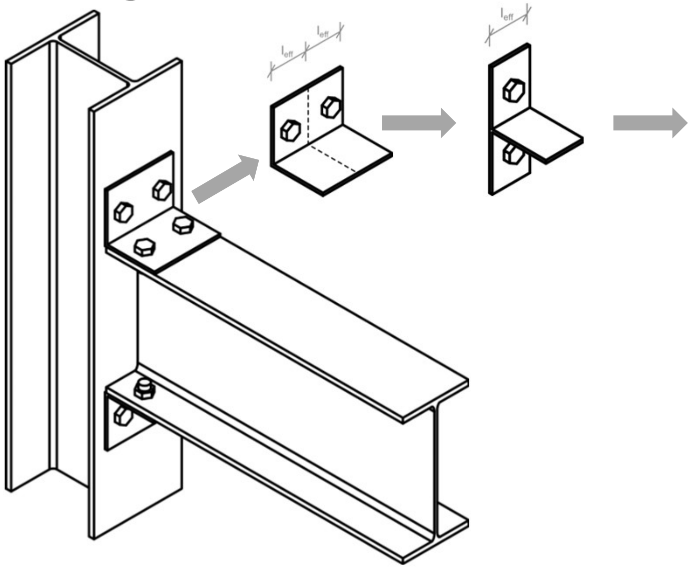

EN 1993-1-8:2024: Equivalent to T-stub in tension

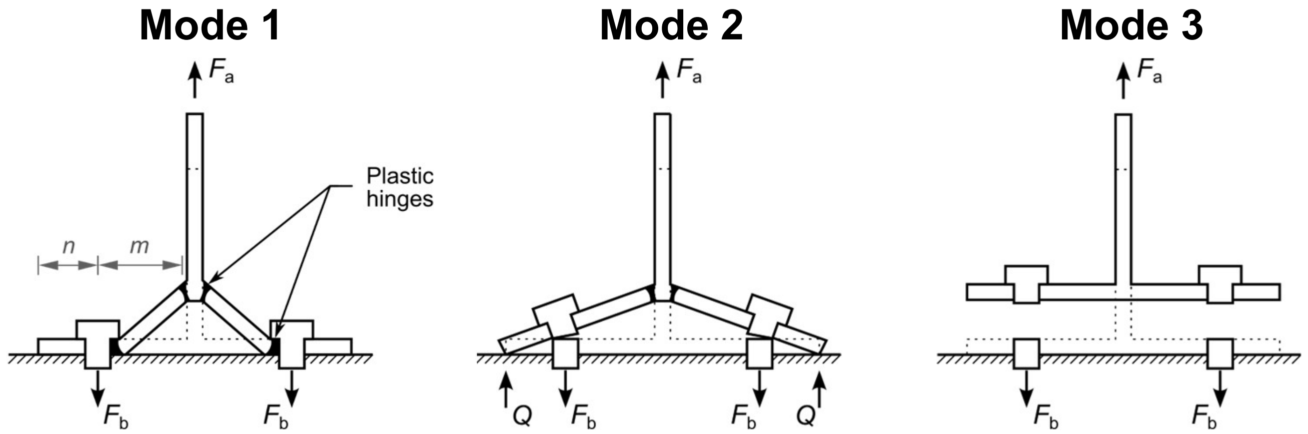

➢ Proposal

Extend failure modes
Predict full-range behaviour
Apply to hybrid steel connections
Cover elevated temperature scenarios

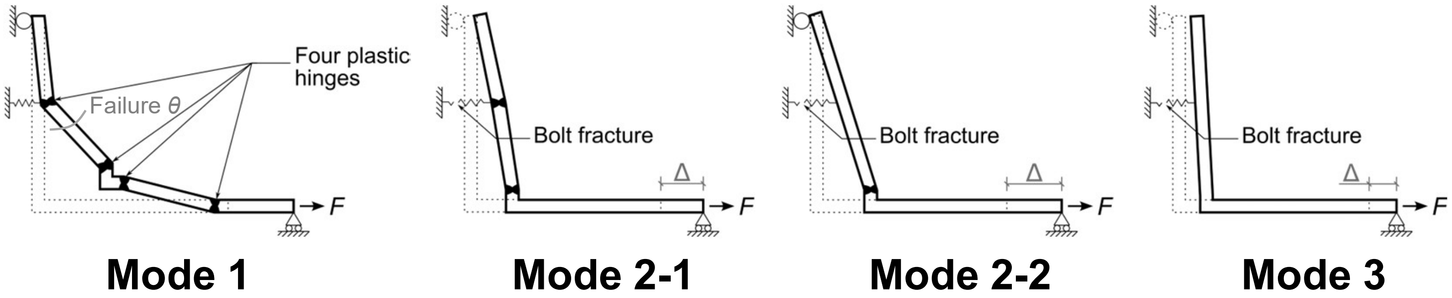

Yan et al., J. Struct. Eng., 2021, 147(1): 04020308:
two further plastic hinges in beam leg
– Mode 1, four hinges (room temperature & ignore bolt extension)

➢ Flow chart

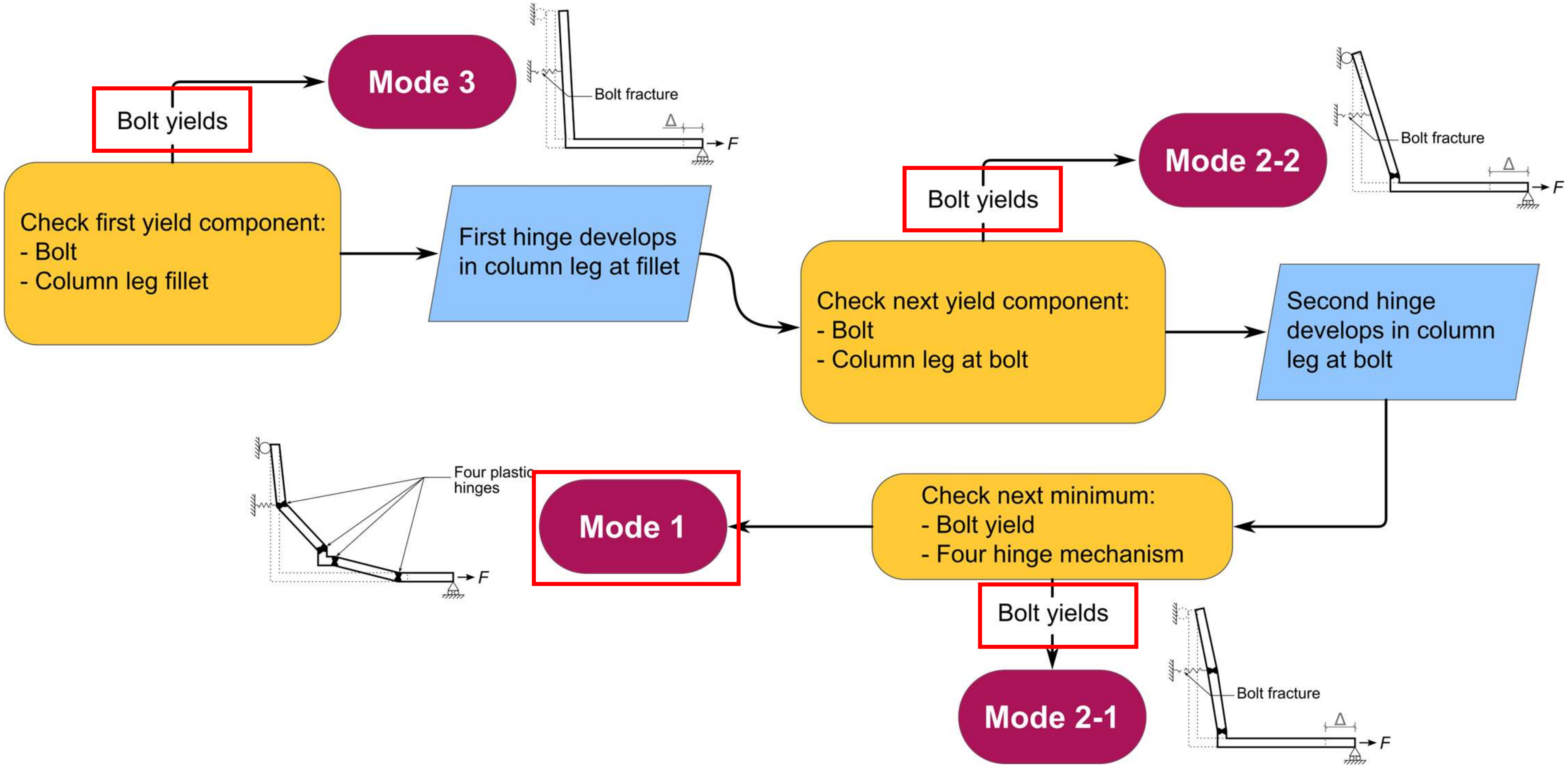
Bolt yields
Mode 3
Bolt fracture
Δ
F
Check first yield component:
- Bolt
- Column leg fillet
First hinge develops in column leg at fillet
Bolt yields
Mode 2-2
Bolt fracture
Δ
F
Check next yield component:
- Bolt
- Column leg at bolt
Second hinge develops in column leg at bolt
Four plastic hinges
F
Mode 1
Check next minimum:
- Bolt yield
- Four hinge mechanism
Bolt yields
Mode 2-1
Bolt fracture
Δ
F

Mode 3

$$K_1 = \frac{12\,E_\mathrm{a}I_\mathrm{a}\,[3E_\mathrm{a}I_\mathrm{a} + k_\mathrm{b}n^2(3L-2n)]}{4L^3[3E_\mathrm{a}I_\mathrm{a} + k_\mathrm{b}n^2(3L-2n)] - k_\mathrm{b}n^2(3L^2-n^2)^2}$$

$$F_1 = \frac{F_\mathrm{y,b}\left[\frac{6E_\mathrm{a}I_\mathrm{a}}{nk_\mathrm{b}} + 2n(3L-2n)\right]}{3L^2-n^2}$$

$$\Delta_1 = \frac{2F_1L^3 - F_\mathrm{y,b}n(3L^2-n^2)}{6E_\mathrm{a}I_\mathrm{a}}$$

$$K_2 = \frac{1}{\frac{1}{k_\mathrm{b,post}} + \frac{m^3}{3E_\mathrm{a}I_\mathrm{a}}}$$

$$F_2 = F_1 + (F_\mathrm{u,b} - F_\mathrm{y,b})$$

$$\Delta_2 = \Delta_1 + \frac{F_2 - F_1}{K_2}$$

- Simple beam theory
- Force & moment equilibrium
- Compatibility of bolt extension & angle deflection

E_a: elastic modulus of angle
I_a: second moment of area of angle
n: distance between prying force and bolt
m: distance between bolt and fillet
L: distance between prying force and fillet
k_b: elastic stiffness of bolt
$k_{b,post}$: post-yielding stiffness of bolt
$F_{y,b}$: bolt yielding strength
$F_{u,b}$: bolt ultimate strength

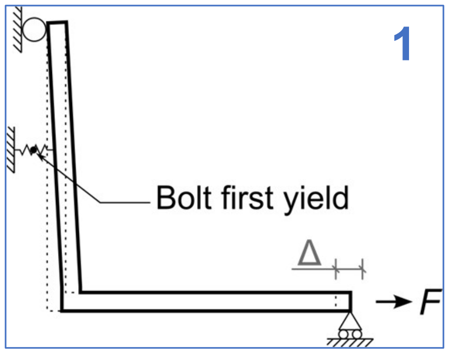

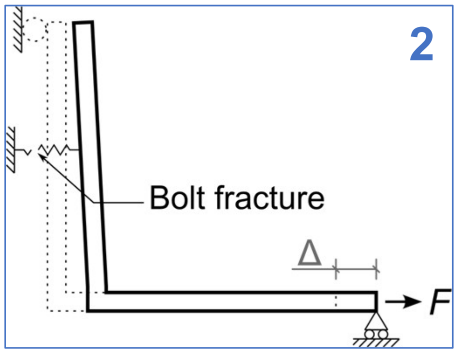

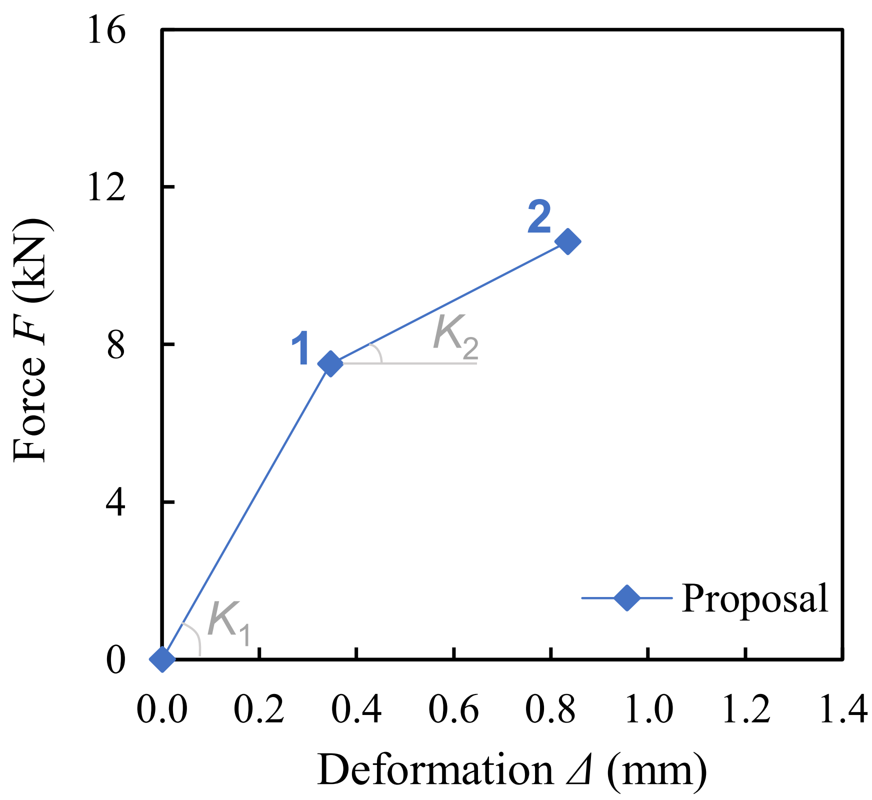

➢ Mode 3

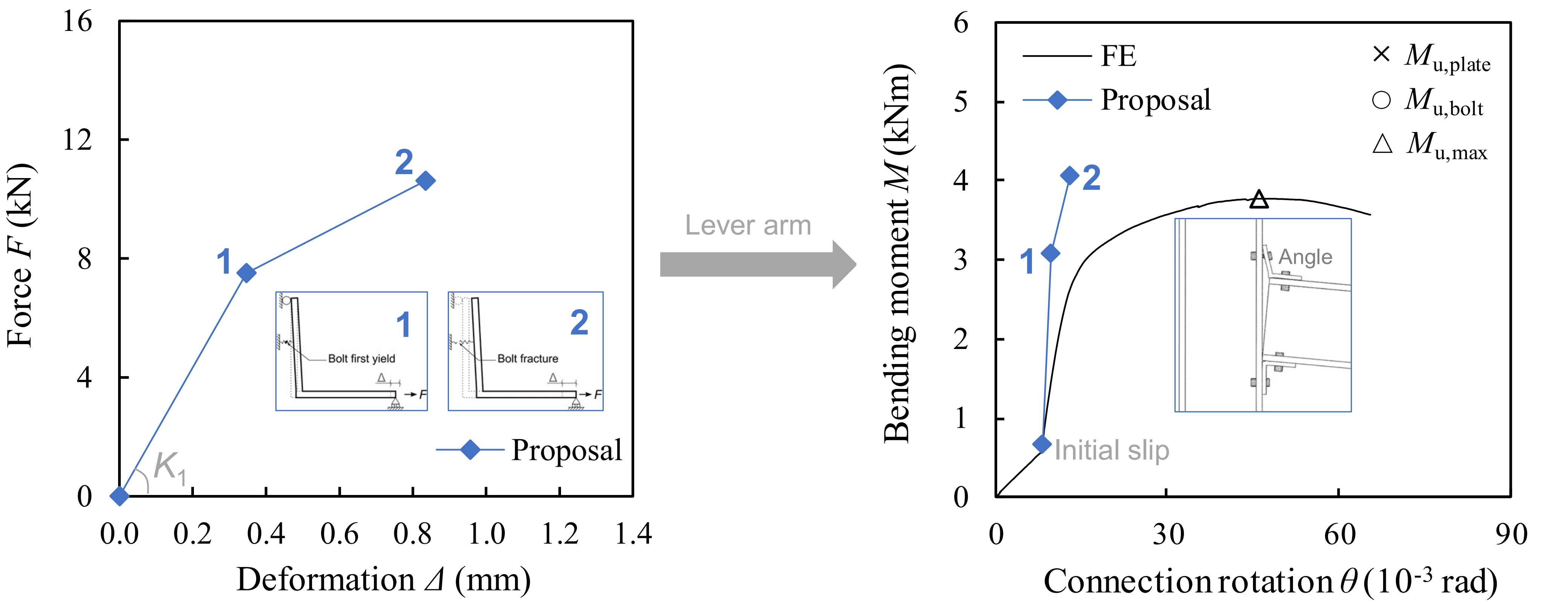

16
12
8
4
0
0.0
0.2
0.4
0.6
0.8
1.0
1.2
1.4
Force F (kN)
Deformation Δ (mm)
1
2
Bolt first yield
Bolt fracture
K1
Proposal
Lever arm
6
5
4
3
2
1
0
0
30
60
90
Bending moment M (kNm)
Connection rotation θ (10-3 rad)
FE
Proposal
Mu,plate
Mu,bolt
Mu,max
Angle
Initial slip

➢ Mode 2-2

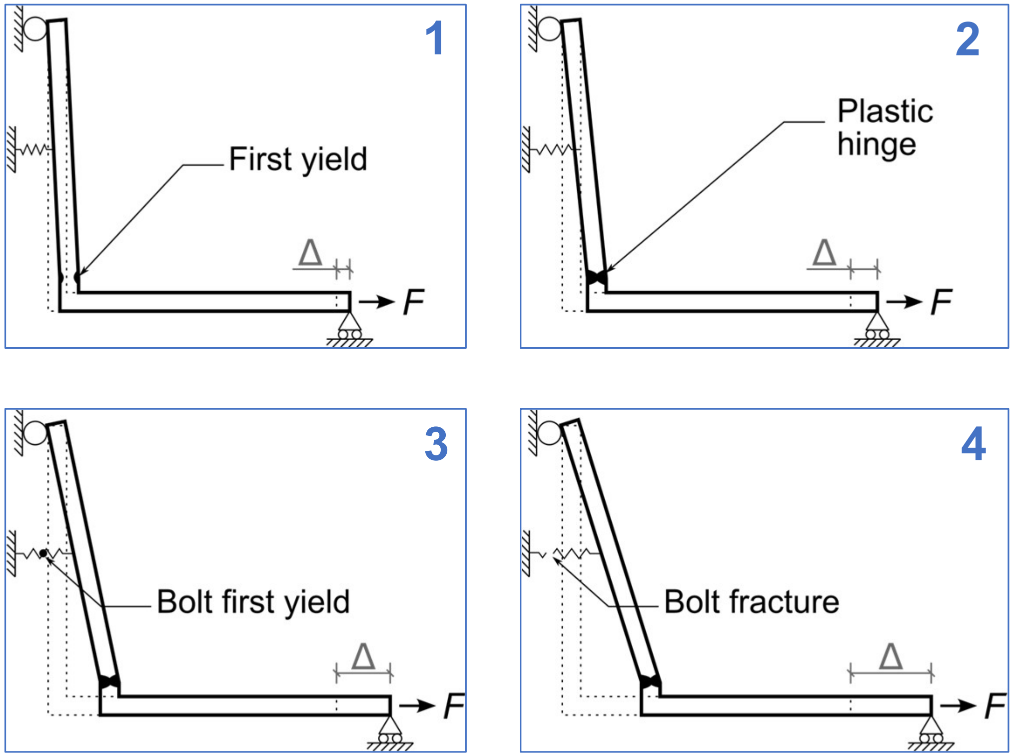
1
First yield
Δ
F
2
Plastic hinge
Δ
F
3
Bolt first yield
Δ
F
4
Bolt fracture
Δ
F

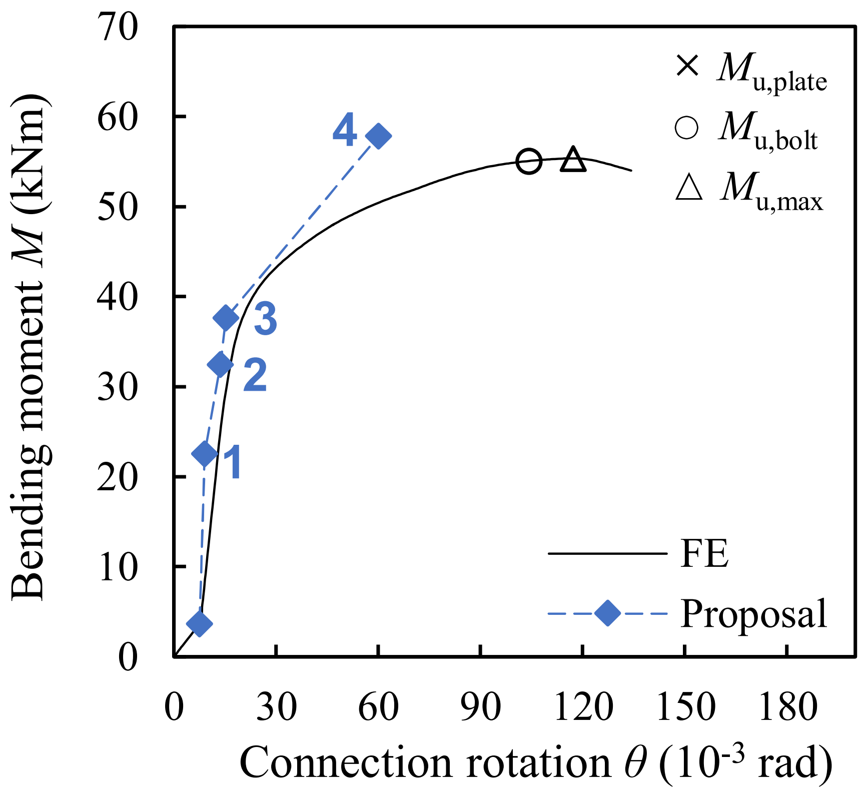
Bending moment M (kNm)
0
10
20
30
40
50
60
70
0
30
60
90
120
150
180
Connection rotation θ (10-3 rad)
M u,plate
M u,bolt
M u,max
FE
Proposal
1
2
3
4

➢ Mode 2-1

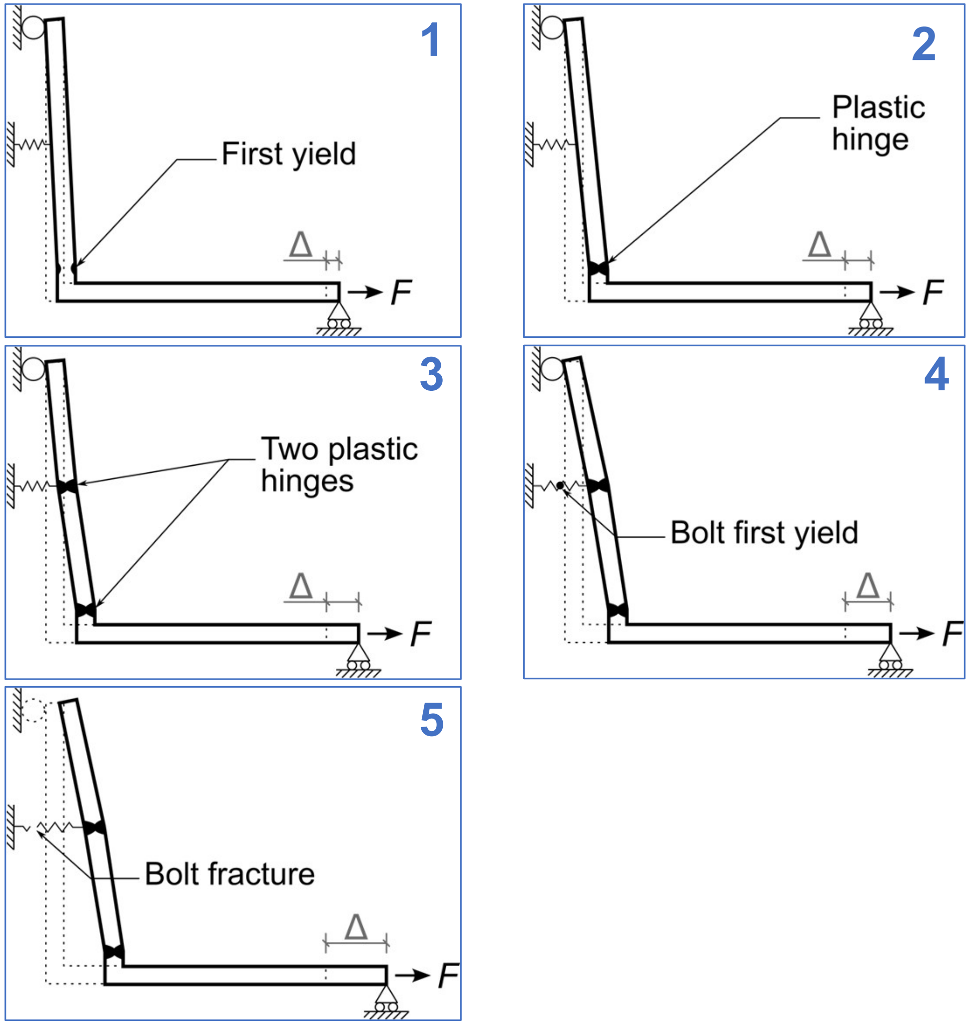
1
First yield
Δ
F
2
Plastic hinge
Δ
F
3
Two plastic hinges
Δ
F
4
Bolt first yield
Δ
F
5
Bolt fracture
Δ
F

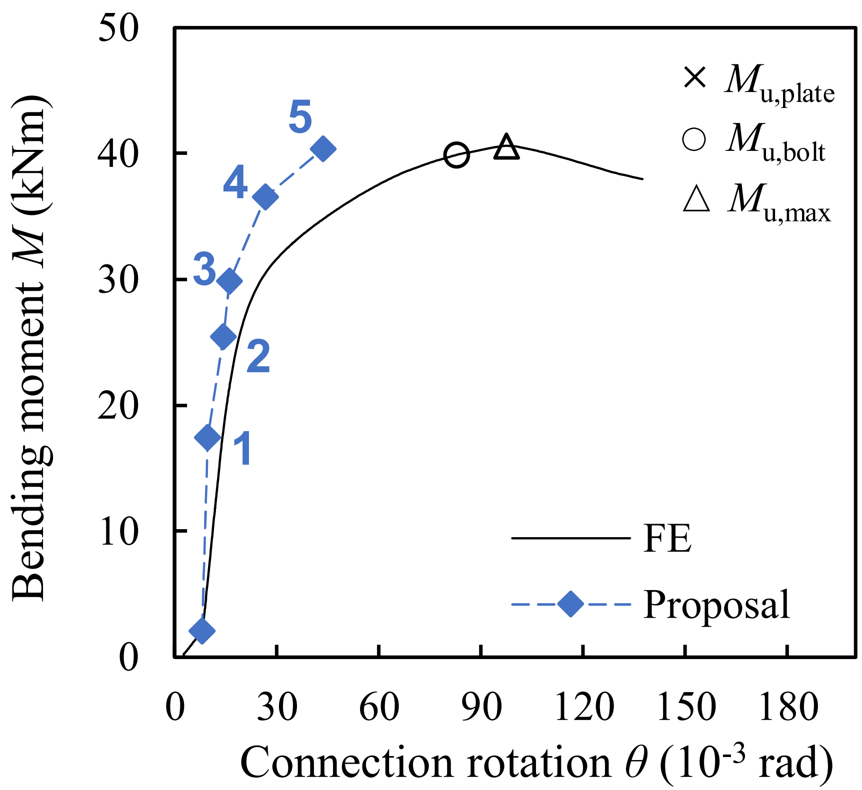
Bending moment M (kNm)
Connection rotation θ (10-3 rad)
0
10
20
30
40
50
0
30
60
90
120
150
180
× M u,plate
○ M u,bolt
△ M u,max
FE
Proposal
1
2
3
4
5

➢ Mode 1

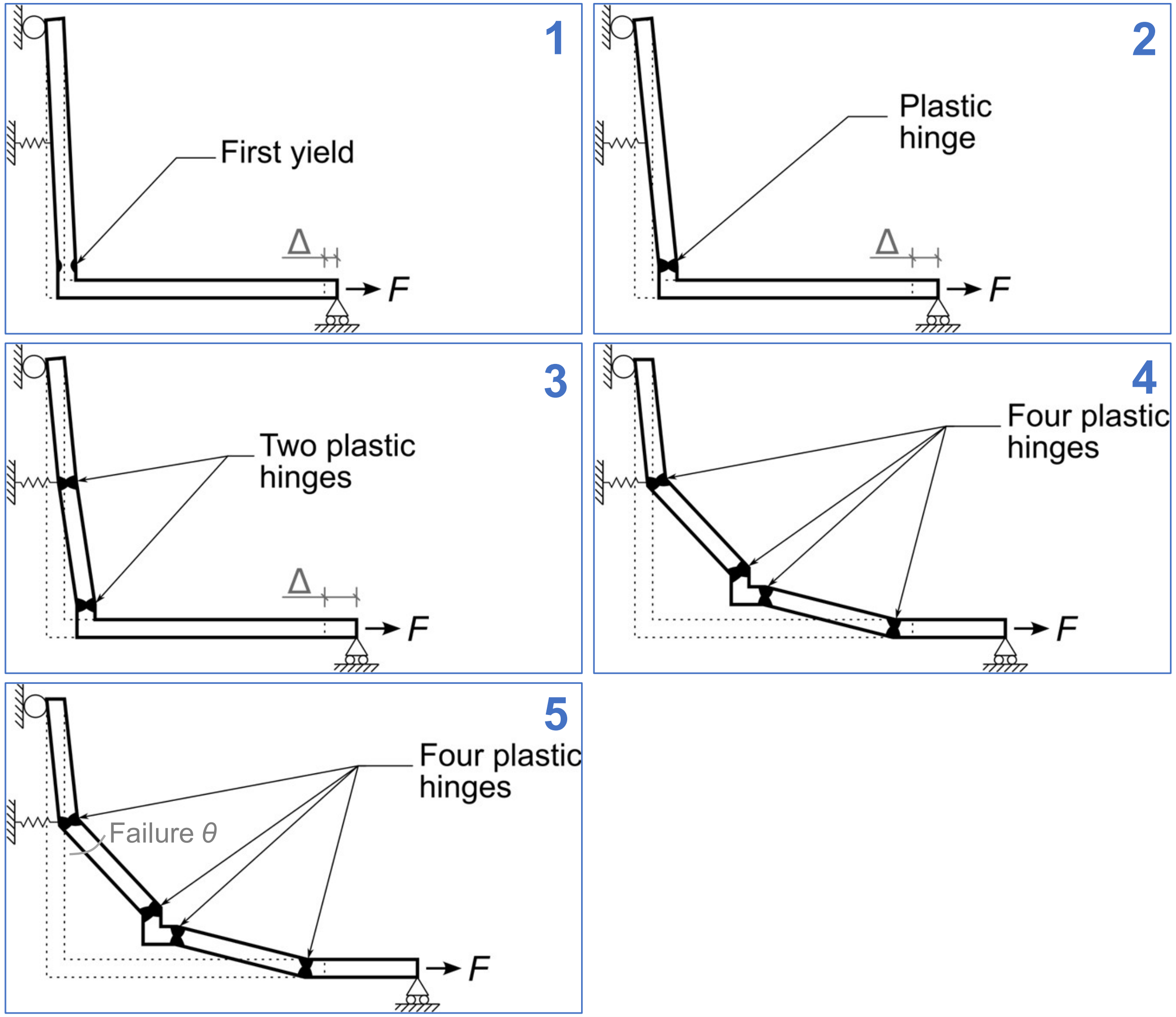
1
First yield
Δ
F
2
Plastic hinge
Δ
F
3
Two plastic hinges
Δ
F
4
Four plastic hinges
F
5
Four plastic hinges
Failure θ
F

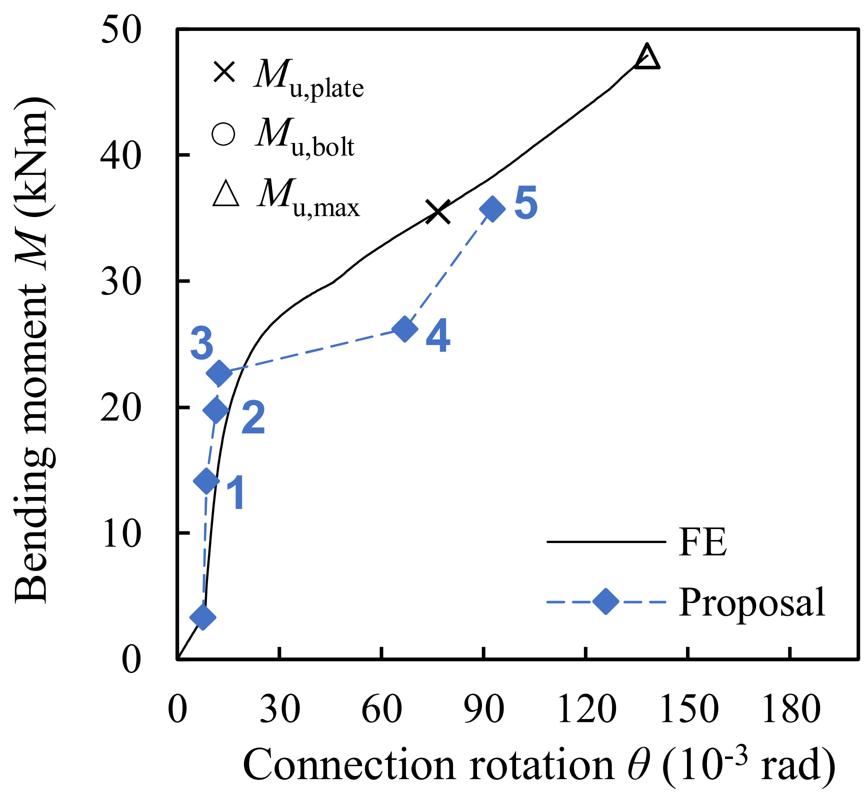
Bending moment M (kNm)
Connection rotation θ (10-3 rad)
0
10
20
30
40
50
0
30
60
90
120
150
180
× M u,plate
○ M u,bolt
△ M u,max
FE
Proposal
1
2
3
4
5

Conclusions

- **EPSRC funded project – RESIlient buildings using STainless steel (RESIST)**
- **Research outcomes – fire and post-fire**

Material properties

✓ Novel stainless steel H500 plates after fire

? Fracture of stainless steel plates and bolts

Connection behaviour

Hybrid: improvements in strength and rotation capacity, especially at higher temperatures

Failure mode may change at different temperatures

Design methodologies

Extend CBM to fire design
Full-range behaviour
Hybrid connections

Stiffness
Resistance
Deformation

Thank you!

<u>Chunyan Quan</u>, Luke Lapira, Katherine A. Cashell

Postdoc Research Fellow

University College London (UCL)

c.quan@ucl.ac.uk

Special thanks to PhD students:
Hadi El Samad
Zhichang Pan